

# End-to-end Active Object Tracking via Reinforcement Learning

Wenhan Luo \* Peng Sun \*  
Tencent AI Lab

wenhanluo, pythonsun@tencent.com

Yadong Mu  
Peking University

muyadong@gmail.com

Wei Liu  
Tencent AI Lab

wliu@ee.columbia.edu

## Abstract

In this paper we propose an active object tracking approach, which provides a tracking solution simultaneously addressing tracking and camera control. Crucially, these two tasks are tackled in an end-to-end manner via reinforcement learning. Specifically, a ConvNet-LSTM function approximator is adopted, which takes as input only visual observations (i.e., frame sequences) and directly outputs camera motions (e.g., move forward, turn left, etc.). The tracker, regarded as an agent, is trained with the A3C algorithm, where we harness an environment augmentation technique and a customized rewarding function to encourage robust object tracking. We carry out experiments on the AI research platform ViZDoom. The yielded tracker can automatically pay attention to the most likely object in the initial frame and perform tracking subsequently, not requiring a manual bounding box as initialization. Moreover, our approach shows a good generalization ability when performing tracking in case of unseen object moving path, object appearance, background and distracting object. The tracker can even restore tracking once it occasionally loses the target.

## 1. Introduction

Object tracking, an important vision problem, has gained much attention in recent decades. The aim of object tracking is to localize an object in continuous video frames given an initial annotation in the first frame. In the setting of most existing work, it is usually assumed that the object of interest is always in the image scene, which means that there is no need to handle camera control during tracking. Namely, the object is tracked in a *passive* fashion. However, passive tracking is not applicable in some cases, e.g., tracking in the case of a camera mounted on a mobile robot and tracking in the application of drone. To this end, one should seek a solution of *active* tracking. Typically, active tracking is tackled by decomposing it into two sub-tasks, i.e., object

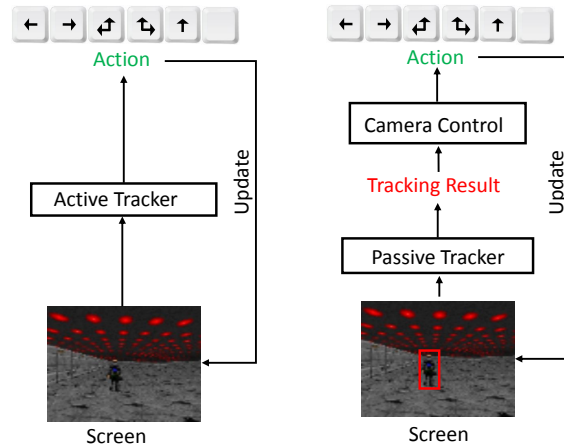


Figure 1. The pipeline of both active tracking (left) and passive tracking (right).

tracking and camera control (see Fig. 1). Additionally, there is a module for the interaction between object tracking and camera control.

Handling these two tasks separately and connecting them by an additional module is not only inelegant but also complicated to jointly tune. Moreover, the mapping from the tracking results to the action of camera control is not trivial. To this end, we propose to tackle this problem in an end-to-end manner, namely, mapping from visual observations to camera action directly (see Fig. 1). To be specific, we train an *active tracker* which is composed of a ConvNet followed by an LSTM unit, taking as input raw video frames and outputting camera movement actions (e.g., move forward, turn left, etc.).

To conveniently simulate active tracking, we adopt the research environment ViZDoom [16, 3]. In this virtual environment, an agent (i.e., the video game player) observes a state (a visual frame) from a first-person perspective and takes an action, and then the environment returns the updated state (next visual frame). We adopt the reinforcement learning algorithm A3C [23] to train the agent (i.e., the tracker). In order to work in the tracking context, a customized rewarding function is designed to encourage the agent to closely follow the object. Also, an environment augmentation technique is proposed to boost the tracker’s

\*Indicate equal contributions

generalization ability. By doing so, an active tracker can be well trained in a relatively short time, typically a few hours.

To our slight surprise, the trained tracker shows a good generalization ability. It performs robust active tracking for unseen object movement paths, object appearance, background and distracting object in the testing stage. Another interesting property of the proposed tracker is its ability of “automatic initialization”: it seeks the most likely object in the first frame and performs tracking of the discovered object in the subsequent frames. Additionally, the tracker can even recover tracking when it occasionally loses the target due to, *e.g.*, abrupt object movement.

In our experiments, our proposed tracking approach also outperforms a few representative traditional passive trackers which are equipped with a hand-tuned camera-control module. Although experimental results of our approach are advanced, our intention is not to replace those traditional passive tracking algorithms. As far as we know, there has not yet been any attempt to deal with active tracking in an end-to-end way. In this work, we investigate it and present its appealing potential. We show that those traditional passive tracking algorithms are not indispensable in active tracking. Alternatively, a direct end-to-end solution can be indeed effective.

## 2. Related Work

As our approach is related to both object tracking and reinforcement learning, we briefly present the related work in these two areas.

### 2.1. Object Tracking

Roughly, object tracking is conducted in both passive and active ways. As mentioned in Sec. 1, passive object tracking has gained more attention due to its relatively simpler problem settings. In the recent decades, passive object tracking has achieved a great progress [35, 38, 22, 34]. Many approaches for object tracking has been proposed to overcome difficulties resulted from issues such as occlusion, illumination variance, and out-of-plane rotation. The seminal work of IVT [26] is one example. Subspace learning is adopted to update the appearance model of the interested object and integrated into a particle filter framework for object tracking. Babenko *et al.* [4] employed multiple instance learning to track an object. Correlation filter based object tracking has also achieved a success in real-time object tracking [5, 13, 19]. In [12], structured output prediction is directly used to constrain object tracking, avoiding the need of converting positions to labels of training samples. These methods have not considered the case when the object disappears and reappears. To this end, tracking, learning and detection are integrated in one framework (called TLD) for long-term object tracking in [15]. Recent years have experienced the success of deep learning in ob-

ject tracking [32, 31]. For instance, a stacked autoencoder is trained to learn good representations for object tracking in [33]. Both low-level and high-level representations are adopted to gain both accuracy and robustness when tracking objects [21].

Active object tracking additionally considers camera control compared against traditional object tracking. There exists not much research attention in the area of active tracking. Conventional solutions deal with object tracking and camera control in separate components [10, 25, 17], but these solutions are difficult to tune. Our proposal is completely different from traditional ones as it tackles object tracking and camera control in an end-to-end manner.

### 2.2. Reinforcement Learning

Reinforcement Learning (RL) intends for a principled approach to temporal decision making problems. In typical RL framework, an *agent* learns from the *environment* a *policy* function that maps *state* to *action* at each discrete time step, where the objective is to maximize the accumulated *rewards* returned by the environment. Let us take robot navigation as an example. The robot itself is an agent and its surroundings constitute the environment. *State* can be either high-level (*e.g.*, the position and the speed of the robot) or low-level (*e.g.*, the raw frame shot from a mounted camera). Action can be discrete movement instruction (*e.g.*, move-forward, turn-left, *etc.*) and the policy can be an arbitrary function model (*e.g.*, a linear function and a neural network). The environment returns a negative reward if the robot hits some obstacle. Historically, RL has been successfully applied to inventory management, path planning, game playing, *etc.* Please refer to [30] for more details.

On the other hand, the past half decade has witnessed a breakthrough in deep learning applied to computer vision tasks, including image classification [18], segmentation [20], object detection and localization [11], and so on. In particular, researchers believe that deep Convolutional Neural Networks (ConvNets) is able to learn good features from raw image pixels, which is able to benefit higher-level tasks.

Equipped with deep ConvNets, RL also shows impressive successes on those tasks involving image (-like) raw states, *e.g.*, playing board game GO [28] and playing video game [24, 36]. Recently, in the computer vision community there are also preliminary attempts of applying deep RL to traditional tasks, *e.g.*, object localization [6] and region proposal [14]. We also note that there exists some methods in RL based visual tracking [7, 37]. However, they are applied to passive tracking, while our focus in this work is active tracking.

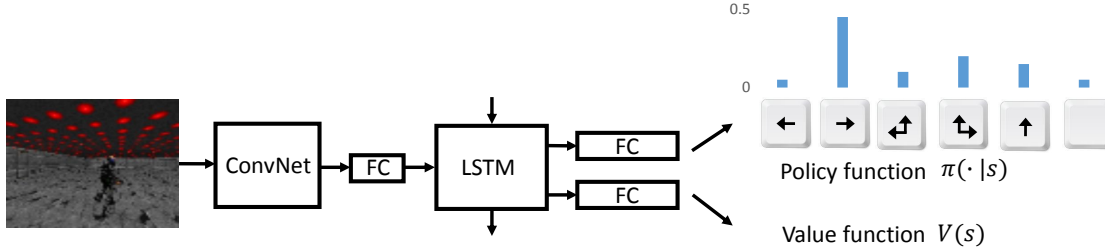


Figure 2. Architecture of the ConvNet-LSTM network.

### 3. Our Approach

In our approach, a tracking scenario is generated based on ViZDoom for both training and testing. To train the tracker, we employ a state-of-the-art reinforcement learning algorithm, A3C [23]. For the sake of robust and effective training, we also propose a data augmentation technique and a customized rewarding function, which are elaborated later.

#### 3.1. ViZDoom

ViZDoom [16] is a deep RL research platform based on a classical 3D First-Person-Shooting video game called Doom. In ViZDoom, the game engine corresponds to the environment, while the video game player corresponds to the agent. The agent receives from the environment a state and a reward at each time step. Although various types of states are available, for a research purpose we let the state be only a RGB screen frame of the first-person perspective in this study.

ViZDoom provides friendly APIs for deep RL research. In particular, it allows customized game maps and scripted monster movements. In this study, we make customized ViZDoom maps (see Fig. 4) composed of object (a monster) and background (ceiling, floor and wall). The monster walks along a pre-specified path programmed by the ACS script [16], and our goal is to train the agent, *i.e.* the tracker, so as to follow closely the object. To be more specific, the tracker observes the raw visual state (RGB screen frame) and takes one action from the action set  $\mathcal{A} = \{\text{turn-left}, \text{turn-right}, \text{turn-left-and-move-forward}, \text{turn-right-and-move-forward}, \text{move-forward}, \text{no-op}\}$ . The action is processed by the environment, which returns to the agent the updated screen frame as well as the current reward.

#### 3.2. A3C Algorithm

Following [23], we adopt a popular RL algorithm called Actor-Critic. At time step  $t$ , we denote by  $s_t$  the observed state, which corresponds to a raw RGB frame. The action set is denoted by  $\mathcal{A}$  of size  $K = |\mathcal{A}|$ . An action,  $a_t \in \mathcal{A}$ , is drawn from a policy function distribution:  $a_t \sim \pi(\cdot|s_t) \in \mathbb{R}^K$ , referred to as an *Actor*. The environment then returns a reward  $r_t \in \mathbb{R}$  according to a *re-*

*warding function*  $r_t = g(s_t)$ , which will be characterized in Sec. 3.4. The updated state  $s_{t+1}$  at next time step  $t + 1$  is subject to a certain but unknown state transition function  $s_{t+1} = f(s_t, a_t)$ , governed by the environment. This way, we can observe a *trace* consisting of a sequence of tuples  $\tau = \{\dots, (s_t, a_t, r_t), (s_{t+1}, a_{t+1}, r_{t+1}), \dots\}$ . Meanwhile, we denote by  $V(s_t) \in \mathbb{R}$  the expected accumulated reward in the future given state  $s_t$  (referred to as *Critic*).

The policy function  $\pi(\cdot)$  and the value function  $V(\cdot)$  are then jointly modeled by a neural network, as will be discussed in Sec. 3.3. Rewriting them as  $\pi(\cdot|s_t; \theta)$  and  $V(s_t; \theta')$  with parameters  $\theta$  and  $\theta'$  respectively, we can learn  $\theta$  and  $\theta'$  over the trace  $\tau$  with simultaneous stochastic policy gradient and value function regression:

$$\theta \leftarrow \theta + \alpha(R_t - V(s_t))\nabla_{\theta} \log \pi(a_t|s_t) + \beta\nabla_{\theta} H(\pi(\cdot|s_t)), \quad (1)$$

$$\theta' \leftarrow \theta' - \alpha(R_t - V(s_t)), \quad (2)$$

where  $R_t = \sum_{t'=t}^{t+T-1} \gamma^{t'-t} r_{t'}$  is a discounted sum of future rewards up to  $T$  time steps with factor  $0 < \gamma \leq 1$ ,  $\alpha$  is the learning rate,  $H(\cdot)$  is an entropy regularizer, and  $\beta$  is the regularizer factor.

During training, several threads are launched, each maintaining an independent environment-agent interaction. However, the network parameters are shared across the threads and updated every  $T$  time steps asynchronously in a lock-free manner using Eq. (1) in each thread. This kind of many-thread training is reported to be fast yet stable, leading to improved generalization [23]. Later in Sec. 3.5, we will introduce an environment augmentation technique to further improve the generalization ability.

#### 3.3. Network Architecture

We train a network as our tracker. As shown in Fig. 2, it is composed of a ConvNet followed by an LSTM unit. Specifically, there are two convolution layers with ReLU in the ConvNet. Features extracted from the ConvNet are flattened and connected with a Fully Connected (FC) layer before being forwarded into the LSTM unit. There are two branches of output after the LSTM unit. One is the policy function  $\pi(\cdot|s_t)$  given by an FC layer and an operation of softmax. The other one is the value function  $V(s_t)$ , given

by another FC layer. Detailed network configurations are as follows,

Layer#	1	2	3	4	5
Parameters	C8×8-16S4	C4×4-32S2	FC256	LSTM256	FC6 FC1

where C8×8-16S4 means 16 filters of size 8×8 and stride 4. FC256 indicates dimension 256. LSTM256 indicates that all the sizes in the LSTM unit are 256.

The screen buffer of ViZDoom is resized to 84 × 84 × 3 RGB image and fed into the network as input. The raw visual information is forwarded and the policy function branch will produce a distribution over  $K = 6$  actions. Finally, an action is drawn from the distribution and received by the environment.

### 3.4. Rewarding Function

To perform active tracking, it is a natural intuition that the rewarding function should encourage the agent to closely follow the object. In this line of thought, firstly we define a two-dimensional local coordinate system, denoted by  $\mathcal{S}$  (see Fig. 3). The  $x$ -axis points from the agent’s left shoulder to his right shoulder, and the  $y$ -axis is perpendicular to the  $x$ -axis and points to the agent’s front. The origin is where the agent is. System  $\mathcal{S}$  is parallel to the floor. Secondly, we manage to obtain object’s local coordinate  $(x, y)$  and orientation  $a$  (in radius) with regard to system  $\mathcal{S}$ .

With a slight abuse of notation, we can now write the rewarding function as

$$r = A - \left( \frac{\sqrt{x^2 + (y - d)^2}}{c} + \lambda|a| \right), \quad (3)$$

where  $A > 0, c > 0, d > 0, \lambda > 0$  are tuning parameters. In plain English, Eq. (3) says that the maximum reward  $A$  is achieved when the object stands perfectly in front of the agent with a distance  $d$  and exhibits no rotation (see Fig. 3).

In Eq. (3) we have omitted the time step subscript  $t$  without loss of clarity. Also note that the rewarding function defined in this way does not explicitly depend on the raw visual state. Instead, it depends on certain internal states. Thanks to the ViZDoom APIs, we are able to access the interested internal states and develop the desired rewarding function.

### 3.5. Environment Augmentation

To make the tracker generalize well at the testing time, we propose a simple yet effective environment augmentation technique for training. Recall the object’s local position and orientation  $(x, y, a)$  in system  $\mathcal{S}$  described in Sec. 3.4. For a given environment (*i.e.*, a ViZDoom map) with initial  $(x, y, a)$ , we randomly perturb it  $N$  times by editing the map with the ACS script [16], yielding a set of environments with varied initial positions and orientations  $\{x_i, y_i, a_i\}_{i=1}^N$ . We further allow flipping left-right the screen frame (and

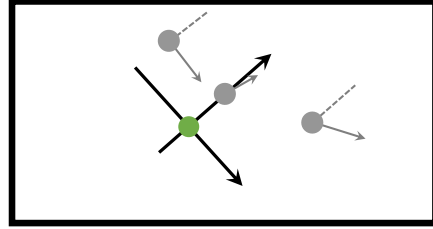


Figure 3. A top view of a ViZDoom map with the local coordinate system. The green dot indicates the agent (tracker). The Gray dot indicates the initial position and orientation of an object to be tracked. Three gray dots mean three possible initial configurations. Arrow indicates the orientation of an object. Dashed gray lines are parallel to the  $y$ -axis. The outer thick black rectangle represents the wall (boundary of the map). Best viewed in color.

accordingly the left-right action). As a result, we obtain  $2N$  environments out of one environment. See Fig. 3 for an illustration of several possible initial positions and orientations in the local system  $\mathcal{S}$ . During the A3C training, we uniformly randomly sample one of the  $2N$  environments at the beginning of every episode. As will be seen in Sec. 4.2, this technique significantly improves the generalization ability of the tracker.

## 4. Experimental Results

The experimental settings is described in Sec. 4.1 and the experimental results are reported in the following. The experiments are carried out in four parts. In the first part (Sec. 4.2), we test the active tracker in a testing environment named *Standard*, showing the effectiveness of the proposed environment augmentation technique. The second part (Sec. 4.3) is contributed to the experiments in more challenging testing environments which vary from the *Standard* testing environment with regard to object appearance, background, object moving path and object distraction. Comparison with a set of traditional trackers is conducted in the third part (Sec. 4.4). Finally, we conduct analysis of what the tracker has learned with a salience visualization technique [29] in the last part (Sec. 4.5).

### 4.1. Settings

**Environment.** A set of environments are generated for both training and testing. For training, we use a small map and this single map is then augmented as described in Sec. 3.5 with  $N = 21$ . We thus randomly sample from up to 42 environments during training. Please see an example named *RandomizedSmall* in top left of Fig. 4. For testing, we make other 9 maps as shown in the rest of Fig. 4. For both training and testing environments, we require that the object be in the first-person view of the agent on initialization, *i.e.*, the object can be “seen” by the agent in the first frame of each episode. In all maps, the path of the object (a ViZDoom monster) is pre-specified, indicated by the blue lines in Fig. 4. However, it is worthy noting that the object does not



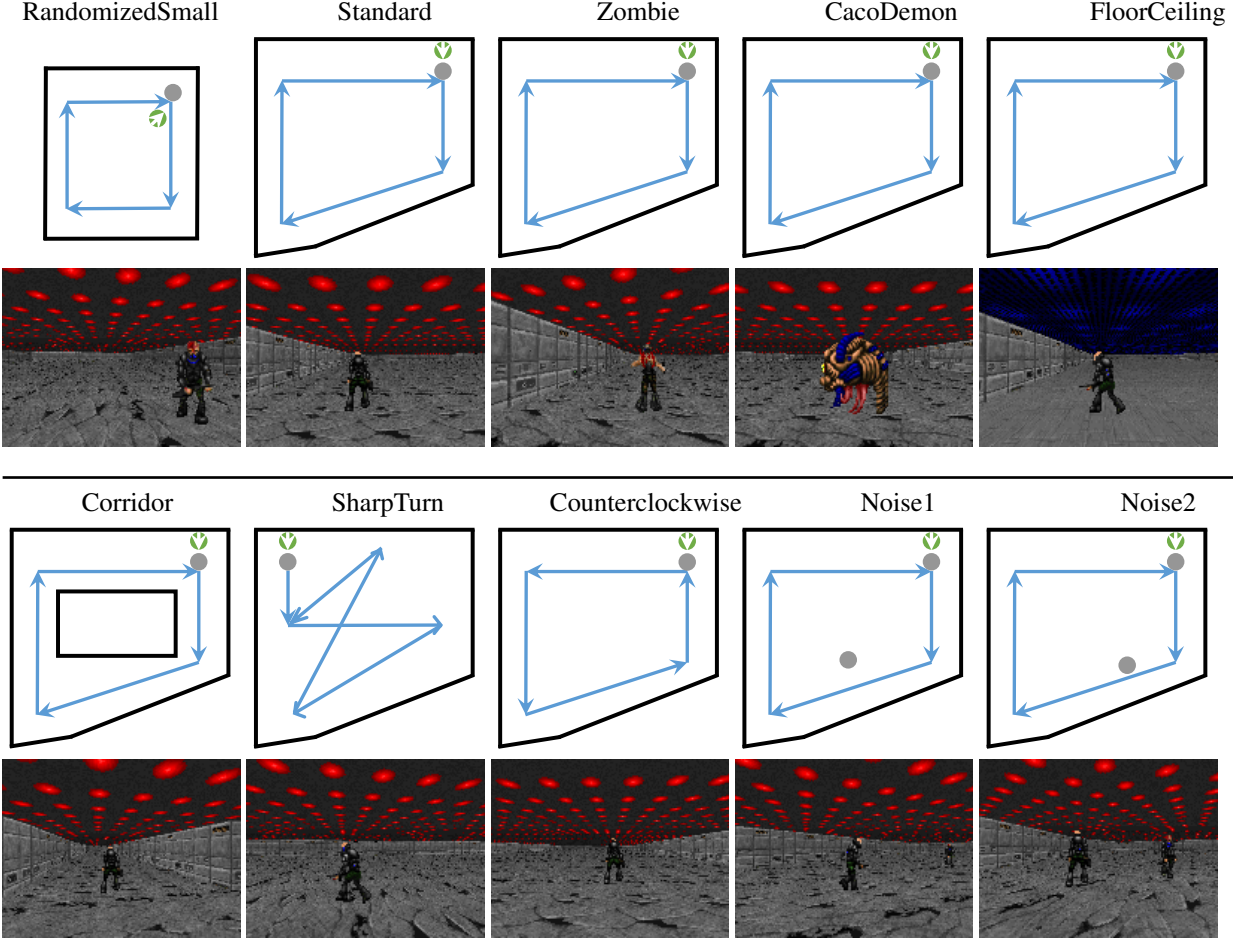


Figure 4. Maps and screenshots of environments. In all maps, the green dot represents the agent. The gray dot indicates the object. Blue lines are planned paths and black lines are walls. Best viewed in color.

strictly follow the planned path. Instead, it sometimes randomly moves in a “zig-zag” way during the course, which is a built-in game engine behavior. This poses an additional difficulty to the tracking problem. For both training and testing, we let each episode be terminated once the accumulated reward reaches -450 or 3000 time steps have passed.

**Metric.** Two metrics are employed for the experiments. Specifically, *Accumulated Reward* (AR) value and *Episode Length* (EL) value of each episode are calculated for quantitative evaluation. In the following, all the experiments are run 100 episodes to report the mean value and the standard deviation value, unless specified otherwise. Note that, the metric of AR plays the role similar to that of *Precision* in traditional tracking, while the EL metric shares the same concept as the metric of *Successfully Tracked Frames* in traditional tracking applications. Also note that the theoretically maximum AR and EL values are both 3000 due to our episode termination criterion when letting  $A = 1.0$  in Eq. (3).

**Implementation details.** The network parameters are updated with Adam optimization, with the initial learning

rate  $\alpha = 0.0001$  in Eq. (1). The regularizer  $\beta = 0.01$  and the reward discount factor  $\gamma = 0.99$ . The parameter updating frequency is  $T = 20$ , and the maximum global iteration for training is  $100 \times 10^6$ . Validation is performed every 70 seconds and the best validation network model is applied to report performance in testing environments.

## 4.2. Active Tracking in Standard Testing Environment

In this part, the proposed active tracker is tested in an environment called *Standard*. This environment is different from the environments we adopt for training. To be specific, the trajectory along which the monster walks is different from that in the training environments. The trajectory in the training stage is a rectangle (*RandomizedSmall* in Fig. 4) while in evaluation that is a quadrangle with acute angle, obtuse angle and right angle (*Standard* in Fig. 4). This is to verify that our tracker does not track the object by memorizing its trajectory.

As described in Sec. 3.5, we perform random sampling from augmented environments for training. We refer this

Table 1. Performance of different protocols in the *Standard* testing environment.

Protocol	AR	EL
<i>RandomizedEnv</i>	2547±58	2959±32
<i>SingleEnv</i>	840±602	2404±287

strategy as *RandomizedEnv* protocol. Alternatively, we also train a tracker by using just one specific map (included in our training maps). This one is referred to as *SingleEnv* protocol. Performance values of both protocols are reported in Tab. 1.

As shown in Tab. 1, the tracker trained with *RandomizedEnv* protocol outperforms that trained with *SingleEnv* protocol significantly. The reason may be that in *RandomizedEnv* protocol multiple random configurations between the target and the agent greatly improve the tracker’s ability of seizing the object in case of acute and obtuse angles. However, without this kind of random configurations, the tracker may easily lose the object in case of acute and obtuse angles which are not present in the training environments. In other words, randomness brought by the proposed environment augmentation technique improves the generalization ability of the tracker.

We examine the training log, and discover that the *SingleEnv* protocol quickly exhausts the training capability and obtains the best validation result at about  $9 \times 10^6$  global iterations. On the contrary, the best validation result of *RandomizedEnv* protocol is obtained after approximately  $48 \times 10^6$  global iterations. Although it spends more time, the potential of the network is well explored. In the following experiments, we only report experiment results with the *RandomizedEnv* protocol.

### 4.3. Active Tracking in Various Testing Environments

To evaluate the generalization ability of our active tracker, we test it in more challenging environments varying from the environment of *Standard*. Specifically, we modify the *Standard* testing environment in the following aspects:

- Change the appearance of object, *i.e.*, the monster in the environment. Specifically, we have two instances. In one instance, we change the object as the monster *Cacodemon*. In the other instance, the monster is replaced by a zombie. We refer these two instances as *CacoDemon* and *Zombie*, respectively (see Fig. 4).
- Revise the background in the environment. In particular, two instances are derived. The first one is obtained by changing the ceiling and the floor of the *Standard* environment. The second one is varied by placing walls as an inner rectangle, forming a corridor structure. These two instances are named as *FloorCeiling* and *Corridor*, respectively (see Fig. 4).

Table 2. Performance of the proposed active tracker in different testing environments.

Environment	AR	EL
<i>CacoDemon</i>	2415±71	2981±10
<i>Zombie</i>	2386±86	2904±40
<i>FloorCeiling</i>	1504 ± 158	2581 ± 84
<i>Corridor</i>	2636 ± 34	2983 ± 17
<i>SharpTurn</i>	2560±34	2987±12
<i>Counterclockwise</i>	2537±58	2964±23
<i>Noise1</i>	2493±72	2977±14
<i>Noise2</i>	2313±103	2855±56

- Modify the path. The original path is altered by a challenging one composed of several sharp acute angles. One more instance is derived by changing the clockwise path to a counterclockwise one. These two instances are termed as *SharpTurn* and *Counterclockwise*, respectively (see Fig. 4).
- Add distractions. We set up two testing environments. More specifically, the first environment is formed by placing a stationary monster on the path along which the target walks. This distracting monster is the same as the object of interest concerning appearance. The second one is the same as the first one except that the distracting monster is closer to the path than that in the first case. These two environments are called as *Noise1* and *Noise2*, respectively (see Fig. 4).

Evaluation performance is reported in Tab. 2.

1) The first set of environments aims to test the sensitivity of our tracker to appearance variations of the target object. Even we replace the target monster with completely different targets (zombie and *Cacodemon*), the corresponding results show that it generalizes well in case of appearance changes.

2) The purpose of the second set is to investigate how the tracker works when the background changes. When we change the ceiling, the floor, or even place additional walls in the map, the results show that the tracker is not sensitive to background variations.

3) In traditional tracking, objects are commonly assumed to move smoothly. The case of abrupt motions is seldom considered. To this end, we also examine the tracker in the *SharpTurn* environment. Even in case of very sharp turns which are abnormal in practical scenes, the tracker can still chase the object tightly. We are suspicious of the performance of traditional passive trackers in this environment.

Additionally, it is observed that the tracker can also recover tracking when it accidentally loses the target. As shown in Fig. 5, the object turns right suddenly from frame #1360 to frame #1361. Consequently, the tracker loses the target (see frame #1372 and #1376). From frame #1376 to #1394, although the target completely disappears from the

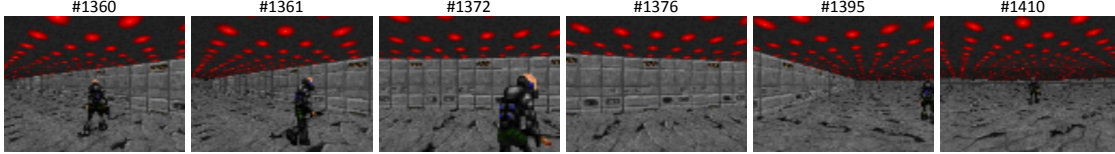


Figure 5. Recovering tracking when the target disappears in the *SharpTurn* environment.

image, the tracker takes a series of *turn-right* actions, until frame #1395, where the tracker discovers the target, and then it quickly follows the target (frame #1410). We believe this capability attributes to the LSTM unit which takes into account historical states when producing current outputs.

In the *Counterclockwise* environment, the tracker is observed to track well when the object walks along a counterclockwise path, which is not present in the training environment. This indicates that the trained tracker does not track the object by memorizing the turning direction.

4) The last set intends to confuse the tracker when object walks along the planned path. In the presence of bait in the *Noise1* environment, the tracker ignores the bait and stably focuses on the object of interest. One may concern the distraction in the *Noise1* environment since the distracting object is kind of far away from the target object. While the performance in the *Noise2* case can dismiss this concern. The object acting as a bait is placed very close to the position the target object will pass. Surprisingly, the tracker does not drift to the distraction and consistently focuses on the target object.

The results in various testing environments reveal that the proposed tracker does not overfit a specific appearance, background or path. It is even robust to distraction. We believe that this benefits from the representation learned from the active ConvNet-LSTM network trained via reinforcement learning. Readers are encouraged to watch more result videos which are available at <https://youtu.be/C1Bn8WGtv0w>.

#### 4.4. Comparison with Simulated Traditional Trackers

In a more extensive experiment we compare the proposed tracker with a few traditional trackers. These trackers are originally developed for passive tracking applications. Particularly, the MIL [4], Meanshift [8], KCF [13], and Correlation [9] trackers are employed for comparison. We implement them by directly invoking the interface from OpenCV [2] (MIL, KCF and Meanshift trackers) and Dlib [1] (Correlation tracker).

To make the comparison feasible, we add to these passive trackers an additional rule-based module for choosing action and thus for interacting with the ViZDoom environment (see Fig. 1). Specifically, the pipeline goes as follows: a passive tracker requires that a manual bounding box be given to indicate the object to be tracked in the first frame. Then it observes the visual frame returned from the environ-

Table 3. Comparison with traditional trackers in the *Standard*, *SharpTurn* and *Cacodemon* environments. The best results are shown in bold.

Environment	Tracker	AR	EL
<i>Standard</i>	MIL	$-454.2 \pm 0.3$	$743.1 \pm 21.4$
	Meanshift	$-452.5 \pm 0.2$	$553.4 \pm 2.2$
	KCF	$-454.1 \pm 0.2$	$228.4 \pm 5.5$
	Correlation	$-453.6 \pm 0.2$	$252.7 \pm 16.6$
	Active	<b><math>2457 \pm 58</math></b>	<b><math>2959 \pm 32</math></b>
<i>SharpTurn</i>	MIL	$-453.3 \pm 0.2$	$388.3 \pm 15.5$
	Meanshift	$-454.4 \pm 0.3$	$250.1 \pm 1.9$
	KCF	$-452.4 \pm 0.2$	$199.2 \pm 5.7$
	Correlation	$-453.0 \pm 0.2$	$186.3 \pm 6.0$
	Active	<b><math>2560 \pm 34</math></b>	<b><math>2987 \pm 12</math></b>
<i>Cacodemon</i>	MIL	$-453.5 \pm 0.2$	$540.6 \pm 18.2$
	Meanshift	$-452.9 \pm 0.2$	$484.3 \pm 9.4$
	KCF	$-454.5 \pm 0.3$	$263.1 \pm 6.2$
	Correlation	$-453.3 \pm 0.2$	$155.8 \pm 1.9$
	Active	<b><math>2451 \pm 71</math></b>	<b><math>2981 \pm 10</math></b>

ment, and outputs the object bounding box as the tracking result. Subsequently, the action-choosing module compares the tracking result of the current frame with that of the previous frame, and estimates how the object moves. It then tries to “pull back” the object to its previous position in the screen by executing a proper action based on a set of hand-tuned rules.

For a fair comparison with the proposed active tracker, we employ the same action set  $\mathcal{A}$  as described in Sec. 3.1. The hand-tuned rules, mapping tracking result to action, are given as follows:

- *Turn-left*: if the object moves to left and does not move forward.
- *Turn-right*: if the object moves to right and does not move forward.
- *Turn-left-and-move-forward*: if the object moves to left and moves forward simultaneously.
- *Turn-right-and-move-forward*: if the object moves to right and moves forward simultaneously.
- *Move-forward*: if the object only moves forward.
- *No-op*: if the object moves “backward”.

Armed with this “camera control” module, the performance of traditional trackers is compared with the active tracker in the testing environments of *Standard*, *SharpTurn* and *Cacodemon*. Evaluation results are reported in Tab. 3.

The results in Tab. 3 show that the end-to-end active tracker beats the simulated “active” trackers by a significant gap. Performance of the Meanshift, KCF and Correlation

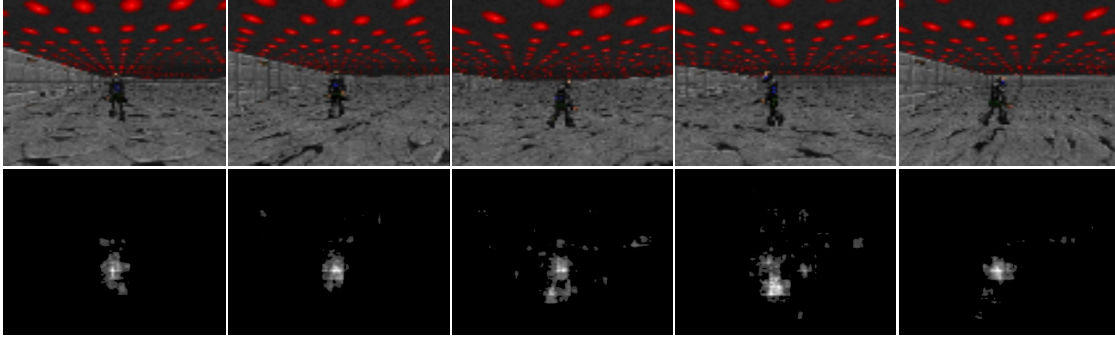


Figure 6. Saliency maps learned by the tracker. The top row shows input observations, and the bottom row shows their corresponding saliency maps. The corresponding actions of these input images are *turn-right-and-move-forward*, *turn-left-and-move-forward*, *turn-left-and-move-forward*, *turn-left-and-move-forward*, and *move-forward*, respectively. These saliency maps clearly show the focus of the tracker.

trackers is worse than that of the MIL tracker. We investigate the tracking process of these trackers and find that these three trackers lose the target object soon. Traditional Meanshift tracker works well when there is no camera shift between continuous frames, while in the active tracking scenario it loses the object soon. Both KCF and Correlation trackers seem not capable of handling such a large camera shift, so they do not work as well as the case in passive tracking. The MIL tracker works reasonably in the active case, while it easily drifts when the object turns suddenly.

Recalling Fig. 5, another reason our tracker beating the traditional trackers is that our tracker can quickly discover the target object again when the object is missed. While the simulated traditional trackers can hardly recover from failure cases.

One may argue that integrating a sophisticated strategy for camera control could improve the performance of traditional passive trackers. We believe that it is true. However, it is non-trivial to fulfill it. One may have to adopt much expertise of Control Science. On the other hand, it is difficult to integrate a tracking module and a camera-control module, and to make them jointly work well. Further discussions in this line of thought are beyond the scope of this paper. To this end, we argue that the end-to-end learning can be an alternation to those problems mentioned above.

#### 4.5. Action Saliency Map

We are curious about what the trained tracker has learned so that it leads to good performance. To this end, we follow the method in [29] to generate a saliency map of the input image with regard to a specific action. Making it more specific, an input frame  $s_i$  is fed into the tracker and forwarded to output the policy function. An action  $a_i$  will be sampled subsequently. Then the gradient of  $a_i$  with regard to  $s_i$  is propagated backwards to the input layer and a saliency map is generated. This process calculates exactly which part of the original input image influences the corresponding action with the greatest magnitude.

Note that the saliency map is image specific, *i.e.*, for each

input image a corresponding saliency map can be derived. Consequently, we can observe how the input images influence the tracker’s actions. Fig. 6 shows a few pairs of input image and corresponding saliency map. The saliency maps consistently show that the pixels corresponding to the object dominate the importance to actions of the tracker. It indicates that the tracker indeed learns how to find the object.

## 5. Remarks

It is very difficult to collect realistic data for active object tracking due to the coupled interaction between the tracker (agent) and its surroundings (environment). Therefore, in this study we leverage a virtual environment, *i.e.*, the ViZDoom, to develop and investigate our end-to-end deep RL solution. Recently, there is a trend of training deep RL in simulated environments for a real-world task, *e.g.*, in-door robot navigation [39] and in-door UAV flight [27]. On the other hand, the success of deep RL is significantly in debt to the image feature expression power of ConvNet, which makes the policy learning on top much easier. Therefore, we are cautiously optimistic that the proposed approach as well as the same network architecture in this study can work well in a more realistic environment and inspire more efforts for end-to-end active object tracking deployed in real-world.

## 6. Conclusion

In this paper, we proposed a tracker for the active tracking scenario. This tracker is trained in an end-to-end fashion via reinforcement learning. A customized rewarding function and a technique of environment augmentation are adopted in the training stage based on the A3C algorithm. The experimental results in the ViZDoom environment verify the effectiveness of the proposed tracker. Adaptions to more practical scenarios would be taken into consideration as a future research direction.



## References

- [1] Dlib. <http://dlib.net/>. Accessed: 2017-03-05. 7
- [2] Opencv. <http://opencv.org/>. Accessed: 2017-03-05. 7
- [3] Vizdoom. <http://vizdoom.cs.put.edu.pl/>. Accessed: 2017-03-05. 1
- [4] B. Babenko, M.-H. Yang, and S. Belongie. Visual tracking with online multiple instance learning. In *Computer Vision and Pattern Recognition*, pages 983–990, 2009. 2, 7
- [5] D. S. Bolme, J. R. Beveridge, B. A. Draper, and Y. M. Lui. Visual object tracking using adaptive correlation filters. In *Computer Vision and Pattern Recognition*, pages 2544–2550, 2010. 2
- [6] J. C. Caicedo and S. Lazebnik. Active object localization with deep reinforcement learning. In *International Conference on Computer Vision*, pages 2488–2496, 2015. 2
- [7] J. Choi, J. Kwon, and K. M. Lee. Visual tracking by reinforced decision making. *arXiv preprint arXiv:1702.06291*, 2017. 2
- [8] D. Comaniciu, V. Ramesh, and P. Meer. Real-time tracking of non-rigid objects using mean shift. In *Computer Vision and Pattern Recognition*, volume 2, pages 142–149, 2000. 7
- [9] M. Danelljan, G. Häger, F. Khan, and M. Felsberg. Accurate scale estimation for robust visual tracking. In *British Machine Vision Conference*, 2014. 7
- [10] J. Denzler and D. W. Paulus. Active motion detection and object tracking. In *International Conference on Image Processing*, volume 3, pages 635–639, 1994. 2
- [11] R. Girshick, J. Donahue, T. Darrell, and J. Malik. Rich feature hierarchies for accurate object detection and semantic segmentation. In *Computer Vision and Pattern Recognition*, 2014. 2
- [12] S. Hare, S. Golodetz, A. Saffari, V. Vineet, M.-M. Cheng, S. L. Hicks, and P. H. Torr. Struck: Structured output tracking with kernels. *IEEE Transactions on Pattern Analysis and Machine Intelligence*, 38(10):2096–2109, 2016. 2
- [13] J. F. Henriques, R. Caseiro, P. Martins, and J. Batista. High-speed tracking with kernelized correlation filters. *IEEE Transactions on Pattern Analysis and Machine Intelligence*, 37(3):583–596, 2015. 2, 7
- [14] Z. Jie, X. Liang, J. Feng, X. Jin, W. Lu, and S. Yan. Tree-structured reinforcement learning for sequential object localization. In *Advances in Neural Information Processing Systems*, pages 127–135, 2016. 2
- [15] Z. Kalal, K. Mikolajczyk, and J. Matas. Tracking-learning-detection. *IEEE Transactions on Pattern Analysis and Machine Intelligence*, 34(7):1409–1422, 2012. 2
- [16] M. Kempka, M. Wydmuch, G. Runc, J. Toczek, and W. Jaśkowski. Vizdoom: A doom-based ai research platform for visual reinforcement learning. *arXiv preprint arXiv:1605.02097*, 2016. 1, 3, 4
- [17] K. K. Kim, S. H. Cho, H. J. Kim, and J. Y. Lee. Detecting and tracking moving object using an active camera. In *International Conference on Advanced Communication Technology*, volume 2, pages 817–820, 2005. 2
- [18] A. Krizhevsky, I. Sutskever, and G. E. Hinton. Imagenet classification with deep convolutional neural networks. In F. Pereira, C. J. C. Burges, L. Bottou, and K. Q. Weinberger, editors, *Advances in Neural Information Processing Systems*, pages 1097–1105, 2012. 2
- [19] T. Liu, G. Wang, and Q. Yang. Real-time part-based visual tracking via adaptive correlation filters. In *Computer Vision and Pattern Recognition*, pages 4902–4912, 2015. 2
- [20] J. Long, E. Shelhamer, and T. Darrell. Fully convolutional networks for semantic segmentation. In *Computer Vision and Pattern Recognition*, pages 3431–3440, 2015. 2
- [21] C. Ma, J.-B. Huang, X. Yang, and M.-H. Yang. Hierarchical convolutional features for visual tracking. In *International Conference on Computer Vision*, pages 3074–3082, 2015. 2
- [22] X. Mei and H. Ling. Robust visual tracking using  $l_1$  minimization. In *International Conference on Computer Vision*, pages 1436–1443, 2009. 2
- [23] V. Mnih, A. P. Badia, M. Mirza, A. Graves, T. P. Lillicrap, T. Harley, D. Silver, and K. Kavukcuoglu. Asynchronous methods for deep reinforcement learning. In *International Conference on Machine Learning*, 2016. 1, 3
- [24] V. Mnih, K. Kavukcuoglu, D. Silver, A. A. Rusu, J. Veness, M. G. Bellemare, A. Graves, M. Riedmiller, A. K. Fidjeland, G. Ostrovski, et al. Human-level control through deep reinforcement learning. *Nature*, 518(7540):529–533, 2015. 2
- [25] D. Murray and A. Basu. Motion tracking with an active camera. *IEEE Transactions on Pattern Analysis and Machine Intelligence*, 16(5):449–459, 1994. 2
- [26] D. A. Ross, J. Lim, R.-S. Lin, and M.-H. Yang. Incremental learning for robust visual tracking. *International Journal of Computer Vision*, 77(1-3):125–141, 2008. 2
- [27] F. Sadeghi and S. Levine. (cad)2rl: Real single-image flight without a single real image. *arXiv preprint arXiv:1611.04201*, 2016. 8
- [28] D. Silver, A. Huang, C. J. Maddison, A. Guez, L. Sifre, G. Van Den Driessche, J. Schrittwieser, I. Antonoglou, V. Panneershelvam, M. Lanctot, et al. Mastering the game of go with deep neural networks and tree search. *Nature*, 529(7587):484–489, 2016. 2
- [29] K. Simonyan, A. Vedaldi, and A. Zisserman. Deep inside convolutional networks: Visualising image classification models and saliency maps. *ICLR*, 2013. 4, 8
- [30] R. S. Sutton and A. G. Barto. *Introduction to Reinforcement Learning*. MIT Press, Cambridge, MA, USA, 1st edition, 1998. 2
- [31] L. Wang, W. Ouyang, X. Wang, and H. Lu. Visual tracking with fully convolutional networks. In *International Conference on Computer Vision*, pages 3119–3127, 2015. 2
- [32] L. Wang, W. Ouyang, X. Wang, and H. Lu. Stct: Sequentially training convolutional networks for visual tracking. In *Computer Vision and Pattern Recognition*, pages 1373–1381, 2016. 2
- [33] N. Wang and D.-Y. Yeung. Learning a deep compact image representation for visual tracking. In *Advances in Neural Information Processing Systems*, pages 809–817, 2013. 2
- [34] X. Wang, G. Hua, and T. X. Han. Discriminative tracking by metric learning. In *European Conference on Computer Vision*, pages 200–214, 2010. 2

- [35] Y. Wu, J. Lim, and M.-H. Yang. Online object tracking: A benchmark. In *Computer Vision and Pattern Recognition*, pages 2411–2418, 2013. [2](#)
- [36] Y. Wu and Y. Tian. Training agent for first-person shooter game with actor-critic curriculum learning. In *ICLR*, 2017. [2](#)
- [37] D. Zhang, H. Maei, X. Wang, and Y.-F. Wang. Deep reinforcement learning for visual object tracking in videos. *arXiv preprint arXiv:1701.08936*, 2017. [2](#)
- [38] K. Zhang, L. Zhang, and M.-H. Yang. Real-time compressive tracking. In *European Conference on Computer Vision*, pages 864–877, 2012. [2](#)
- [39] Y. Zhu, R. Mottaghi, E. Kolve, J. J. Lim, A. Gupta, L. Fei-Fei, and A. Farhadi. Target-driven visual navigation in indoor scenes using deep reinforcement learning. *ICRA*, 2017. [8](#)